J|A|C|S ARTICLES

Published on Web 10/01/2009

Homogeneous Deposition of Platinum Nanoparticles on Carbon Black for Proton Exchange Membrane Fuel Cell

Baizeng Fang, Nitin K. Chaudhari, Min-Sik Kim, Jung Ho Kim, and Jong-Sung Yu*

Department of Advanced Materials Chemistry, BK21 Research Team, Korea University, 208 Seochang, Jochiwon, ChungNam 339-700, Republic of Korea

Received July 11, 2009; E-mail: jsyu212@korea.ac.kr

Abstract: A simple and efficient approach has been developed for synthesis of carbon-supported Pt nanoparticles (NPs) that combines homogeneous deposition (HD) of Pt complex species through a gradual increase of pH realized by *in situ* hydrolysis of urea and subsequent uniform reduction by ethylene glycol (EG) in a polyol process, giving control over the size and dispersion of Pt NPs. With increasing amount of urea in the starting Pt salt aqueous solution, the size of Pt complex species decreases and so does that of the metallic Pt NPs. The decrease in size of the Pt species is likely attributable to two determining factors: the steric contraction effect and the electrostatic charge effect. The excellent electrocatalysis ability of the Pt catalysts produced by HD-EG is demonstrated through the determination of electrochemical surface area and fuel-cell polarization performance. The Pt NPs deposited on Vulcan XC-72 (VC) carbon black by the HD-EG strategy show smaller size with more uniform dispersion, higher Pt utilization efficiency, and considerably improved fuel-cell polarization performance compared with the Pt NPs prepared by conventional sodium borohydride reduction or by a microwave-assisted polyol approach. Particularly important and significant is that this HD-EG method is very efficient for the synthesis of high Pt loading catalysts with tunable NP size and uniform particle dispersion. A high metal loading catalyst such as Pt(60 wt %)/VC fabricated by the HD-EG method outperforms ones with mid-to-low metal loadings (i.e., 40 and 20 wt %), even at a very low catalyst loading of 0.2 mg of Pt cm^{-2} at the cathode, which is for the first time reported for the VC-supported Pt catalysts.

1. Introduction

Platinum is an excellent and versatile catalyst for diverse important chemical /electrochemical reactions, especially those that take place at low temperature, but it occurs at a very low level of abundance in nature, resulting in prohibitive cost for Pt-based catalysts. Therefore, further enhancement of their catalytic activity and utilization efficiency has long been of fundamental importance.[1,2] To date, a great deal of research and effort has been focused on the development of strategies to produce Pt-based catalysts with a high surface area for high catalytic activity and utilization efficiency.[3,4]

Hydrogen is the most abundant element in the universe, and it can be produced easily from renewable energy sources; thus, it represents an important alternative energy feedstock. Particularly when hydrogen is combined with fuel-cell technology, very high energy conversion efficiency can be achieved.[5] For these reasons, proton exchange membrane fuel cells (PEMFCs) exclusively represent the most advanced fuel-cell technology[1,5] and have been of great interest as future energy sources for applications such as low/zero-emission electric vehicles, distributed home power generators, and power sources for small, portable electronics.[6,7] However, the commercialization of PEMFCs technology has been greatly hindered by some challenges, mainly sluggish kinetics of the oxygen reduction reaction (ORR) and the high cost of Pt-based catalysts.[8,9]

Catalyst support technology has been proved to be a very effective approach to improve the catalytic activity of Pt-based catalysts,[10−12] reduce the Pt usage in catalysts, and thus lower the fuel-cell cost. Although diverse carbon materials have been explored as catalyst supports, such as Vulcan XC-72R carbon black (VC),[13−15] carbon nanotubes (CNTs),[16,17] and carbon

(1) Tian, N.; Zhou, Z.-Y.; Sun, S.-G.; Ding, Y.; Wang, Z.-L. *Science* **2007**, *316*, 732–735.
(2) Lee, H.; Habas, S. E.; Somorjai, G. A.; Yang, P. *J. Am. Chem. Soc.* **2008**, *130*, 5406–5407.
(3) Ahmadi, T. S.; Wang, Z. L.; Green, T. C.; Henglein, A.; El-Sayed, M. A. *Science* **1996**, *272*, 1924–1925.
(4) Bönnemann, H. B.; Kfner, N. W. *Chem. Mater.* **2002**, *14*, 1115–1120.
(5) Borup, R.; Meyers, J.; Pivovar, B.; Kim, Y. S.; Mukundan, R.; Garland, N.; Myers, D.; Wilson, M.; Garzon, F.; Wood, D. *Chem. Rev.* **2007**, *107*, 3904–3951.
(6) Service, R. *Science* **2002**, *296*, 1222–1224.
(7) Huang, Y.; Wang, A.; Li, L.; Wang, X.; Su, D.; Zhang, T. *J. Catal.* **2008**, *255*, 144–152.
(8) Fang, B.; Kim, J. H.; Lee, C.-G.; Yu, J.-S. *J. Phys. Chem. C* **2008**, *112*, 639–645.
(9) Fang, B.; Kim, J. H.; Kim, M. S.; Yu, J.-S. *Chem. Mater.* **2009**, *21*, 789–796.
(10) Yu, J.-S.; Kang, S.; Yoon, S. B.; Chai, G. S. *J. Am. Chem. Soc.* **2002**, *124*, 9382–9383.
(11) Chai, G. S.; Shin, I. S.; Yu, J.-S. *Adv. Mater.* **2004**, *16*, 2057–2061.
(12) Fang, B.; Kim, M. S.; Yu, J.-S. *Appl. Catal. B: Environ.* **2008**, *84*, 100–105.
(13) Qu, Z.; Huang, W.; Zhou, S.; Zheng, H.; Liu, X.; Cheng, M.; Bao, X. *J. Catal.* **2005**, *234*, 33–36.
(14) Li, W.; Liang, C.; Zhou, W.; Qiu, J.; Zhou, Z. H.; Sun, G.; Xin, Q. *J. Phys. Chem. B* **2003**, *107*, 6292–6299.
(15) Okamoto, M.; Fujigaya, T.; Nakashima, N. *Small* **2009**, *5*, 735–740.
(16) Zheng, S.-F.; Hu, J.-S.; Zhong, L.-S.; Wan, L.-J.; Song, W.-G. *J. Phys. Chem. C* **2007**, *111*, 11174–11179.

10.1021/ja905749e CCC: $40.75

nanofibers (CNFs),[18] VC is still the most commonly used catalyst support in PEMFCs because of its wide commercial availability, relatively large surface area, and excellent chemical stability in the fuel-cell environment.

Generally, the Pt loading of Pt/VC catalysts is between 20 and 60 wt %. The lower the Pt loading is, the thicker the electrode catalyst layer has to be for the same Pt usage on the electrode. In that case, mass transport of reactants (fuel and O_2/air) and products in the electrode is limited. Therefore, it is particularly important to use catalysts with high Pt loading. Unfortunately, the preparation of Pt/VC catalysts with high Pt loading becomes much more difficult due to the agglomeration of Pt nanoparticles (NPs). Legratiet et al. reported a significant increase in the size of Pt NPs for commercial E-TEK Pt/VC catalysts, namely, a Pt NP is 2.0 nm in Pt(10 wt %)/VC, 3.2 nm in Pt(30 wt %)/VC, and 8.8 nm in Pt(60 wt %)/VC.[19]

The catalytic activity of the metal is strongly dependent on the particle size, dispersion, and size distribution.[20] Synthesis of highly dispersed supported platinum with uniform NP size is highly desired but still remains a challenge, especially for high metal loading. To date, various synthesis strategies have been developed, such as wet impregnation−borohydride reduction,[21,22] colloidal methods,[23,24] and a microemulsion method.[25] Although these methods have been widely used to synthesize supported Pt catalysts with low metal loading (i.e., 20 wt % Pt), allowing a narrow particle size distribution in the range of 1−5 nm, the methods either do not provide adequate control over particle size and distribution for preparing carbon-supported catalysts with high Pt loading (i.e., higher than 40 wt % Pt)[19] or are very complex, time-consuming (requiring additional procedures to remove the residual protective agent), and costly.

A polyol process using ethylene glycol (EG) as a precursor of the reducing agent has been widely used recently[26−28] since its first use by Yu and co-workers,[26] in which conductive heating or microwave (MW) dielectric loss heating (i.e., irradiation) was utilized to *in situ* generate species of reducing agent. Compared with the impregnation−$NaBH_4$ reduction method, the polyol process has demonstrated an enhanced ability for partial control over the particle size and dispersion of the supported metal NPs due to its rapid and homogeneous *in situ* generation of reducing species, resulting in more uniform metal deposition on the support. However, pH adjustment prior to the chemical reduction step (i.e., polyol process) was usually realized through external addition of an alkaline solution such as aqueous KOH, which may result in a local increase of the pH value and fast precipitation of metal hydroxide, particularly in the case of high metal loading, which would accordingly give large particle size with uneven particle distribution.[9] pH value has been found to be a key parameter in controlling particle size, shape, and dispersion,[27−31] which play very important roles in the catalytic activity and utilization of nanoscale catalysts. For example, by using cetyltrimethylammonium bromide as capping agent/stabilizer, monodisperse Pt NPs with particle size of ca. 2.5 nm and 3D dendritic Pt nanoclusters with particle size of ca. 40−70 nm were produced at pH $\approx$ 7 and 1.7, respectively.[29]

Urea has been used recently as a precursor of precipitating agent in the preparation of oxide-supported Au catalysts for organic reactions,[32] unsupported metal oxide NPs,[33] SBA-15-supported Pt for toluene hydrogenation,[34] and CNF-supported platinum and ruthenium catalysts with low metal loadings (less than 5 wt %).[35] The urea-assisted homogeneous deposition−precipitation method permits the *in situ* gradual and homogeneous generation of hydroxide ions throughout the whole solution through the urea hydrolysis reaction, taking place above 90 °C, which can avoid local supersaturation and precipitation.[36] The active phase or its precursor is slowly and homogeneously deposited onto an existing support by the precipitating hydroxide ions in such a way that nucleation in the solution itself is avoided.[34] Precipitation takes place only onto the support because of the chemical interaction between the metal species and the support.[36]

On the basis of the analysis mentioned above, and keeping in mind applicability to industrial scales, we developed a facile, efficient, and "green" synthesis strategy, HD-EG, for preparation of VC-supported high metal loading Pt catalysts. The HD-EG method presented in this study combines the advantage of the urea-assisted HD approach, reflected by *in situ* pH value adjustment/control through hydrolysis of urea, with the advantage of the polyol process, namely, rapid, homogeneous *in situ* generation of reducing species for the complete reduction of deposited metal species, and is hence supposed to produce supported Pt catalysts with desired particle size and distribution. The pH value adjustment can be realized by varying the amount of urea added into the starting solution instead of external addition of alkaline solution. Compared with a reduction process conducted under hydrogen flow at higher temperature (i.e., 200 °C),[35] the one-pot reduction of metal species by a polyol process conducted at lower temperature (i.e., lower than 130 °C) in solution not only makes the synthesis of the supported catalysts simpler and more efficient but also enables high loading of metal to be deposited on the support, which is of particular importance for fuel-cell catalysts. Furthermore, the increase in size and agglomeration of Pt NPs caused by high temperatures can be avoided. In our HD-EG strategy, conductive heating was

(17) Wang, C.; Waje, M.; Wang, X.; Tang, J. M.; Haddon, R. C.; Yan, Y. *Nano Lett.* **2004**, *4*, 345–348.
(18) Yuan, F. L.; Ryu, H. *Nanotechnology* **2004**, *15*, s596–s602.
(19) Le Gatiet, B.; Remita, H.; Picq, G.; Delcourt, M. O. *J. Catal.* **1996**, *164*, 36–43.
(20) Liu, H.; Song, C.; Zhang, L.; Zhang, J.; Wang, H.; Wilkinson, D. P. *J. Power Sources* **2006**, *155*, 95–110.
(21) Steigerwalt, E. S.; Deluga, G. A.; Lukehart, C. M. *J. Phys. Chem. B* **2002**, *106*, 760–766.
(22) Chai, G. S.; Yu, J.-S. *J. Mater. Chem.* **2009**, *19*, 6842–6848.
(23) Chan, K.-Y.; Ding, J.; Ren, J.; Cheng, S.; Tsang, K. Y. *J. Mater. Chem.* **2004**, *14*, 505–516.
(24) Bock, C.; Paquet, C.; Couillard, M.; Botton, G. A.; MacDougall, B. R. *J. Am. Chem. Soc.* **2004**, *126*, 8028–8029.
(25) Yeung, C. M. Y.; Yu, K. M. K.; Fu, Q. J.; Thompsett, D.; Petch, M. I.; Tsang, S. C. *J. Am. Chem. Soc.* **2005**, *127*, 18010–18011.
(26) Yu, W.-Y.; Tu, W.-X.; Liu, H.-F. *Langmuir* **1999**, *15*, 6–9.
(27) Liu, Z.-L.; Lee, J.-Y.; Chen, W.-X.; Han, M.; Gan, L.-M. *Langmuir* **2004**, *20*, 181–187.
(28) Chen, Z.-W.; Xu, L.-B.; Li, W.-Z.; Waje, M.; Yan, Y. *Nanotechnology* **2006**, *17*, 5254–5259.
(29) Ullah, M. H.; Chung, W.-S.; Kim, I.; Ha, C.-S. *Small* **2006**, *2*, 870–873.
(30) Ji, X.-H.; Song, X.-N.; Li, J.; Bai, Y.-B.; Yang, W. S.; Peng, X.-G. *J. Am. Chem. Soc.* **2007**, *129*, 13939–13941.
(31) Briñas, R. P.; Hu, M.-H.; Qian, L.-P.; Lymar, E. S.; Hainfeld, J. F. *J. Am. Chem. Soc.* **2008**, *130*, 975–976.
(32) Patil, N. S.; Uphade, B. S.; Jana, P.; Bharagava, S. K.; Choudhary, V. R. *J. Catal.* **2004**, *223*, 236–239.
(33) Wang, H.; Fan, Y.; Shi, G.; Liu, Z.; Liu, H.; Bao, X. *Catal. Today* **2007**, *125*, 149–154.
(34) Chytil, S.; Glomm, W. R.; Kvande, I.; Zhao, T.-J.; Walmsley, J. C.; Blekkan, E. A. *Top. Catal.* **2007**, *45*, 93–99.
(35) Toebes, M. L.; van der Lee, M. K.; Tang, L. M.; Huis in't Veld, M. H.; Bitter, J. H.; van Dillen, A. J.; de Jong, K. P. *J. Phys. Chem. B* **2004**, *108*, 11611–11619.
(36) Burattin, P.; Che, M.; Louis, C. *J. Phys. Chem. B* **1998**, *102*, 2722–2732.

employed in the polyol process instead of MW heating for scalable synthesis of the catalysts. Compared with catalysts synthesized by commonly used impregnation−$NaBH_4$ reduction or MW-assisted polyol processes, the VC-supported Pt catalysts prepared by the HD-EG approach have smaller Pt NPs and more uniform particle distribution, and they demonstrated improved utilization efficiency, considerably enhanced catalytic activity toward ORR, and considerably enhanced fuel-cell polarization performance.

2. Experimental Section

2.1. Synthesis of VC-Supported Pt Catalysts. VC-supported Pt catalysts with various metal loadings of 20−60 wt % were prepared by different synthesis strategies, namely, $NaBH_4$ reduction,[8] microwave-assisted EG (i.e., EG-MW),[9] and urea-assisted EG (i.e., HD-EG) processes. All chemicals were used as received. For each synthesis approach, 200 mL of DI water was used, and 5 mL of 0.05 M $H_2PtCl_6 \cdot 6H_2O$ aqueous solution was added. For synthesis of Pt catalysts with different metal loadings, the required amount of VC was added.

In a HD-EG synthesis, in order to examine the effect of urea amount on the size and distribution of Pt(IV) complex species deposited on the VC after the HD step and Pt NPs of Pt(60 wt %)/VC catalysts, molar ratios of urea to Pt were varied from 0 to 80, corresponding to 0−1200 mg of urea. To compare the catalytic properties of the Pt(60 wt %)/VC catalysts synthesized by various strategies, the HD-EG catalyst was produced with a molar ratio of urea to Pt of 20.

For a typical synthesis of Pt(60 wt %)/VC catalyst by $NaBH_4$ reduction, 32.5 mg of carbon was added into 200 mL of DI water and sonicated for 30 min. Next, 5 mL of 0.05 M $H_2PtCl_6 \cdot 6H_2O$ aqueous solution was added. After stirring for 3 h, the mixture was adjusted to pH 7−8 by dropwise addition of 0.4 M KOH. The $NaBH_4$ aqueous solution was then added dropwise fashion (the molar ratio of $NaBH_4$ to Pt was set at 10). After stirring overnight, the mixture was filtered, and the catalyst residue was washed with copious amounts of water. The resultant Pt catalyst was dried at 80 °C overnight.

For EG-MW synthesis of the Pt(60 wt %)/VC, 32.5 mg of carbon was dispersed in 200 mL of DI water and sonicated for 30 min, followed by addition of 5 mL of 0.05 M $H_2PtCl_6 \cdot 6H_2O$ aqueous solution. After stirring for 3 h, 200 mL of EG was added, and the mixture was adjusted to pH 7−8 by dropwise addition of 0.4 M KOH. The resultant solution was heated in a household microwave oven (National NN-S327WF, 2450 MHz, 700 W) for 5 min. After stirring overnight, the catalyst slurry was filtered, and the residue was washed with copious amounts of water. The collected Pt catalyst was dried at 80 °C overnight.

For a typical HD-EG synthesis of Pt(60 wt %)/VC, 300 mg of urea (i.e., molar ratio of urea/Pt = 20) was dissolved in 200 mL of DI water, 32.5 mg of carbon was added, and the mixture was sonicated for 30 min. Next, 5 mL of 0.05 M $H_2PtCl_6 \cdot 6H_2O$ aqueous solution was added. After stirring for 3 h, the mixture was heated to 90 °C to cause urea hydrolysis and kept for 1 h. The mixture was cooled to room temperature, and 200 mL of EG was added. After stirring for 3 h, the solution was heated to 120 °C, kept for 1 h, and stirred overnight. The catalyst slurry was filtered and washed with copious amounts of water. The resultant Pt catalyst was dried at 80 °C overnight.

Pt/VC catalysts with different Pt loadings, namely, 10, 40, and 60 wt %, were similarly synthesized by various strategies. Actual metal loadings of the VC-supported Pt catalysts were roughly determined by thermogravimetric analysis (TGA).

2.2. Surface Characterization. High-resolution scanning electron microscopy (HRSEM) images were obtained using a Hitachi S-5500 microscope operated at 30 kV. High-resolution transmission electron microscopy (HRTEM) images were obtained using a JEOL FE-2010 microscope operated at 200 kV. X-ray diffraction (XRD) patterns were obtained on a Rigaku 1200 instrument by using Cu Kα radiation and a Ni β-filter, operating at 40 kV and 20 mA. X-ray photoelectron spectroscopy (XPS) analyses were carried out with an AXIS-NOVA (Kratos) X-ray photoelectron spectrometer using a monochromated Al Kα (150W) source under a base pressure of 2.6×10^{-9} Torr.

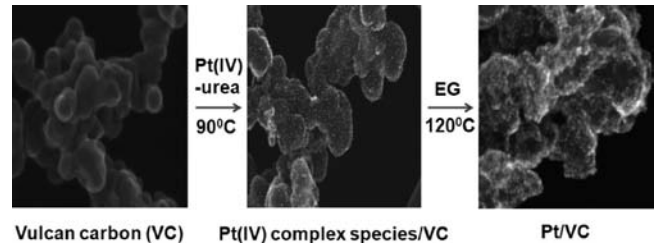

Figure 1. Schematic illustration of the HD-EG strategy for synthesis of VC-supported Pt catalysts.

2.3. Preparation of Catalyst Electrodes and Cell Performance Tests. For determination of electrochemical surface area (ECSA) of Pt in various Pt(60 wt %)/VC catalysts, a three-electrode electrochemical cell (i.e., half-cell) was employed, and cyclic voltammetric (CV) measurements were conducted at room temperature in 0.5 M H_2SO_4 with a scan rate of 25 mV/s. Pt gauze was used as counter electrode and Ag/AgCl as reference electrode. Electrolyte solution was deaerated by high-purity nitrogen for 1 h prior to any CV measurement. Stable voltammograms were recorded after 10 cycles. The working electrode was a thin layer of Nafion-impregnated catalyst cast on a glassy carbon disk of 3 mm diameter embedded in a Teflon cylinder. The catalyst layer was fabricated as follows: 5 mg of Pt catalyst was dispersed in 1 mL of a solution of deionized water and ethanol (1:4 in volume ratio) and then mixed with 50 μL of Nafion solution (5 wt % Nafion). After stirring by ultrasonication for 1 h, 4 μL of catalyst slurry was pipetted and spread on the top of a glassy carbon disk. The catalyst-coated glassy carbon electrode was dried at 80 °C for 2 h to yield a loading of 50 μg of Pt/cm^2. For evaluation of the fuel-cell polarization performance of various Pt catalysts, single cells were constructed. Membrane electrode assembly (MEA) with an area of 6.25 cm^2 was employed to construct a single cell, which had been fabricated by hot-pressing a pretreated Nafion 112 membrane (DuPont) between the anode and cathode. The catalyst loading was 0.4 mg of Pt/cm^2 at the anode and 0.2 mg of Pt cm^{-2} at the cathode. For all the tests, Pt (20 wt %)/VC (E-TEK) was used as anode catalyst. Catalyst inks were prepared by dispersing various Pt/VC catalysts into a mixture solution composed of an appropriate amount of DI water and the required amount of 5 wt % Nafion ionomer solution (Aldrich). The Nafion ionomer content was 20 wt % in the anode catalyst layer and 25 wt % in the cathode. Appropriate amount of the catalyst inks were painted uniformly on Teflon-coated carbon paper (TGPH-090) and dried at 80 °C overnight. Fuel-cell polarization performance tests were conducted at 60 °C under constant current or constant voltage with a WFCTS fuel-cell test station. After the cell was humidified at 75 °C, H_2 and O_2 were supplied to the anode and cathode at a flow rate of 200 and 500 mL min^{-1}, respectively.

3. Results and Discussion

3.1. Pt Loading on VC by HD-EG with Various Amounts of Urea. For urea-assisted HD-EG synthesis of Pt/VC catalysts, the amount of urea added in the starting solution is supposed to play a key role in controlling the size and distribution of Pt(IV) complex species and Pt NPs to be deposited on the VC. A simple schematic illustration of the HD-EG strategy is shown in Figure 1. During the first step, i.e., the urea-assisted HD process, the urea in the acidic Pt salt solution hydrolyzes at a

temperature above 90 °C to generate OH^- gradually and homogeneously throughout the solution.[36] Thus, sudden local pH increase and precipitation of Pt hydroxide in the solution are avoided.

$$CO(NH_2)_2 + 3H_2O \rightarrow 2NH_4^+ + CO_2 + 2OH^- \quad (1)$$

In an acidic solution with low pH, chloroplatinic acid (i.e., H_2PtCl_6) is mainly present as $[PtCl_6]^{2-}$ and $[PtCl_{6-x}(H_2O)_x]^{(2-x)-}$ ($x = 0, 1, 2$), generated through the following reaction:[37]

$$[PtCl_6]^{2-} + xH_2O \leftrightarrow [PtCl_{6-x}(H_2O)_x]^{(2-x)-} + xCl^- \quad (2)$$

When OH^- is added (or generated *in situ*), the following reactions will take place:[37]

$$[PtCl_{6-x}(H_2O)_x]^{(2-x)-} + yOH^- \leftrightarrow [PtCl_{6-x}(OH)_y(H_2O)_{x-y}]^{(2-x+y)-} + yH_2O \qquad (x \geq y) \quad (3)$$

or

$$[PtCl_{6-x}(H_2O)_x]^{(2-x)-} + zOH^- \leftrightarrow [PtCl_{6-x-z}(OH)_z(H_2O)_x]^{(2-x)-} + zCl^- \quad (4)$$

Thus, for a urea-assisted HD process, the species and sizes of the Pt(IV) complexes deposited on the VC depend greatly on the concentration of OH^- generated in reaction 1, and accordingly on the amount of urea added in the starting solution.

During the second step, i.e., EG reducing process, the deposited Pt complex species are reduced to metallic Pt NPs by the reducing agent generated *in situ* by EG at a temperature of over 100 °C through the following reactions:[38,39]

$$CH_2OH{-}CH_2OH \rightarrow CH_3CHO + H_2O \quad (5)$$

$$4CH_3CHO + [PtCl_{6-x-z}(OH)_z(H_2O)_x]^{(2-x)-} + (8 - z)OH^- \rightarrow 4CH_3COO^- + (x + 4)H_2O + Pt + (6 - x - z)Cl^- \quad (6)$$

Apparently, the size and distribution of Pt NPs produced in the reduction process depend heavily on those of the deposited Pt complex species in the HD process and, thus, the amount of urea added in the starting solution.

pH values are shown against the amounts of urea in the starting solution in Figure 2 (top). The pH values for solution series 1 were recorded in the VC slurry solutions in the absence of Pt salt after the hydrolysis of urea at 90 °C for 1 h, while the pH values for solution series 2 were recorded in the presence of Pt salt under the same conditions. It is clear that, in both cases, pH values increase with increasing amount of urea in the starting solution. In a natural VC solution without addition of urea, the pH is ca. 6.68, and after addition of 1.2 g of urea and hydrolysis at 90 °C, the pH increases to 8.23.

For the Pt salt−VC solutions, pH values in the after-HD step solutions also show a monotonic increase with increasing amount of urea, indicating an increase of OH^- produced through urea hydrolysis as shown in eq 1. In our synthesis experiments,

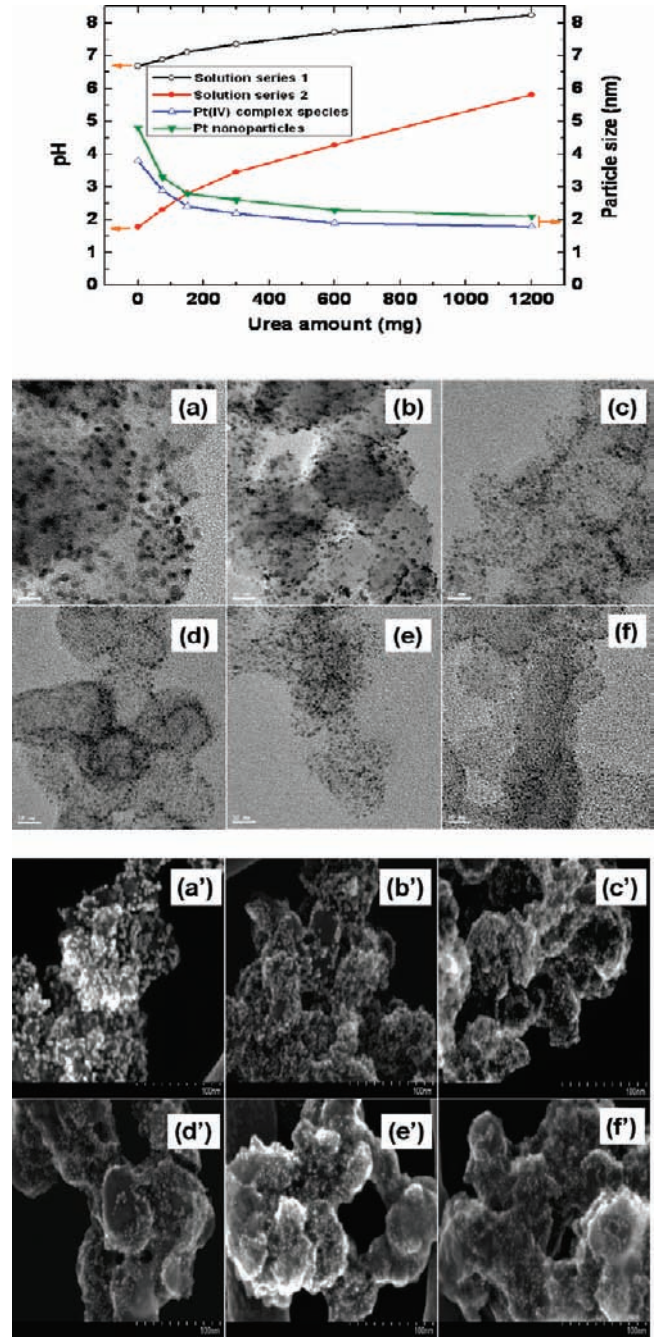

Figure 2. (Top) pH values and sizes of Pt(IV) complex species and metal NPs versus amount of urea for a fixed amount of 48.8 mg of Pt in 200 mL of aqueous solution. (Middle, a−f) HRTEM images for Pt(IV) complex species/VC. (Bottom, a′−f′) HRSEM images for Pt(60 wt %)/VC catalysts. The following amounts of urea were present (mg): 0 (a,a′), 75 (b,b′), 150 (c,c′), 300 (d,d′), 600 (e,e′), and 1200 (f,f′). Solution series 1: VC solutions. Solution series 2: Pt-VC solutions. Scale bar: 10 nm for a−f and 100 nm for a′−f′.

it was observed that all the filtrates were colorless after the HD step, implying that all the Pt complex species were deposited on the VC through the impregnation and interaction between the Pt species and the VC support. The sizes of the Pt complex species and the sizes of Pt NPs deposited on the VC, estimated from their corresponding HRTEM/SEM images shown in Figure 2 (middle and bottom), are plotted against the urea amount in Figure 2 (top). The sizes of both Pt complex species and Pt NPs were found to decrease with increasing amount of urea. The estimated sizes of metal Pt NPs at different amounts of

(37) Spieker, W. A.; Liu, J.; Miller, J. T.; Kropf, A. J.; Regalbuto, J. R. *Appl. Catal. A−Gen.* **2002**, *232*, 219–235.
(38) Komarneni, S.; Li, D.-S.; Newalkar, B.; Katsuki, H.; Bhalla, A. S. *Langmuir* **2002**, *18*, 5959–5962.
(39) Li, X.; Chen, W.-X.; Zhao, J.; Xing, W.; Xu, Z.-D. *Carbon* **2005**, *43*, 2168–2174.

added urea are also in good agreement with those calculated from their XRD patterns (Figure S1, Supporting Information). It is interesting to notice that the Pt(IV) complex species possess clearly observable sizes, as shown in TEM images. Particularly, in the absence of urea in the starting solution, Pt complex species show much larger particulate size and more severe agglomeration compared with Pt complex species obtained in the presence of urea, indicating urea plays an important role in controlling particulate size of Pt complex species. The XPS analysis shown in Figure S2 (Supporting Information) for the deposited Pt complex species on VC reveals that the dominant Pt complex species is Pt(IV) after the urea-assisted HD step, implying that urea's main role is as supplier of OH^-, not reducing agent. On the basis of the TEM images observed in the Figure 2, a significant portion of Pt(IV) complex species likely exists as Pt ionic cluster species, which will need further characterization in future work.

The decreasing size of the deposited Pt complex species with increasing amount of urea is probably attributable to two factors: a steric contraction effect and an electrostatic charge effect. The steric contraction effect results from the substitution of H_2O and/or Cl^- in $[PtCl_{6-x}(H_2O)_x]^{(2-x)-}$ by OH^-, which has a smaller ionic radius (1.32 Å) than the former (i.e., ca. 3.38 Å van der Waals radius for H_2O and 1.81 Å for Cl^-). $[PtCl_{6-x}(OH)_y(H_2O)_{x-y}]^{(2-x+y)-}$ or $[PtCl_{6-x-z}(OH)_z(H_2O)_x]^{(2-x)-}$ is thus supposed to be smaller than $[PtCl_{6-x}(H_2O)_x]^{(2-x)-}$. Chen et al. reported, after a careful EXAFS analysis, that the Pt−Cl distance in $[PtCl_6]^{2-}$ is 2.32 Å and the Pt−O distance in $[PtCl_4(OH)_2]^{2-}$ is 2.03 Å,[40] confirming the steric contraction of $[PtCl_6]^{2-}$ complex species caused by the replacement of Cl^- by OH^-. The electrostatic charge effect can be explained as follows. The net charge for $[PtCl_{6-x}(H_2O)_x]^{(2-x)-}$ is calculated to be -1 if $x = 1$ (i.e., in a very acidic solution, one H_2O molecule has been introduced into the Pt complex species, as shown in eq 2), whereas at higher pH (i.e., with addition of urea), $[PtCl_{6-x}(H_2O)_x]^{(2-x)-}$ can be converted to $[PtCl_{6-x}(OH)_y(H_2O)_{x-y}]^{(2-x+y)-}$, as shown in eq 3, which has a net charge of $2-$ if $y = 1$ and $x = 1$ (i.e., one H_2O in the former Pt complex species was replaced by one OH^-). That is to say, the latter Pt complex species are more negatively charged than the former (at lower pH), and their growth is limited by the stronger electrostatic repulsive interaction; accordingly, only smaller and denser Pt complex species are formed on the VC. Although the two effects may contribute to the small size of Pt(IV) complex species, from their working mechanisms, the "electrostatic charge effect" seems to have a greater impact than the "steric contraction effect" on the distribution of Pt(IV) complex species.

Evidently, in the HD-EG synthesis strategy, the urea-assisted HD step is crucial and dominant in determining the size and dispersion of Pt complex species, while the subsequent EG reduction process further guarantees the formation of small and uniform Pt NPs on the VC. As we will discuss later, other reduction processes, such as $NaBH_4$ or heat treatment in H_2 flow, cannot effectively prevent small Pt NPs from agglomerating into large ones, and thus the uniform distribution of Pt NPs with small size cannot be guaranteed.

Although the question of which Pt complex species dominates at different pH values needs further investigation, the in-depth characterization work carried out in the present paper, in parallel with available literature data, gives some keys to rationalize the effect of urea on the size and dispersion of the Pt complex species deposited on the VC and the effecting mechanism in the first instance. Eventually, the decrease in the particulate size of clearly observed Pt complex species with increasing urea amount and pH value could provide us with the most direct evidence for the deposition of stable Pt complex species on the carbon support and the positive effect (i.e., the decrease in the particulate size) of the increasing urea amount.

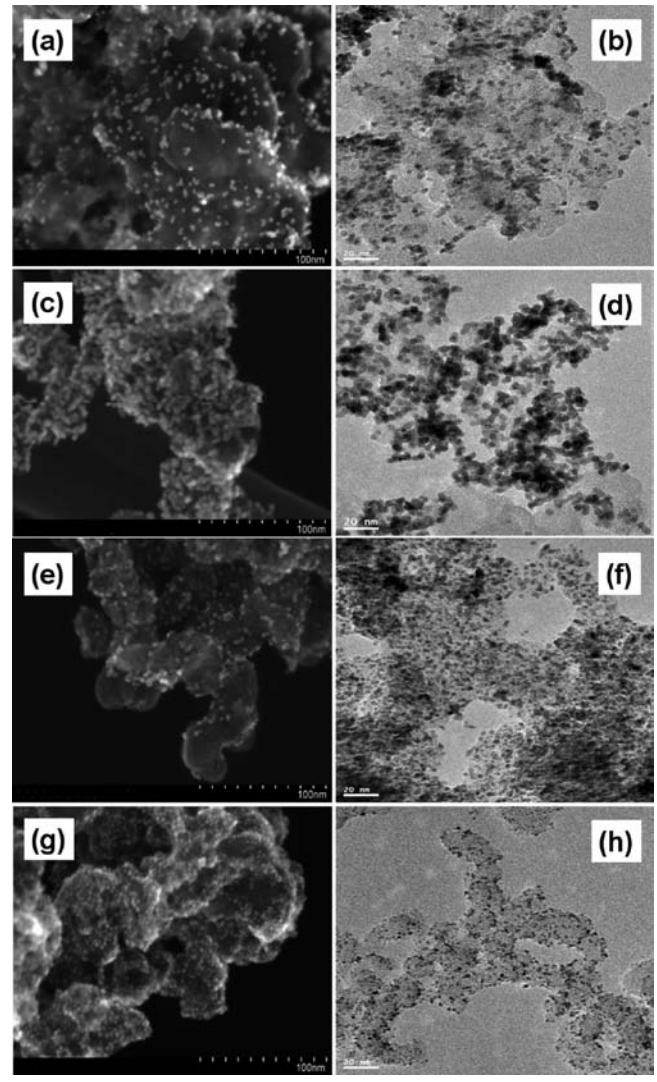

Figure 3. HRSEM and HRTEM images for the Pt(60 wt %)/VC catalysts prepared by the different methods: $NaBH_4$ (a,b), EG-MW (c,d), JM (e,f), and HD-EG (g,h).

3.2. Pt Loading on VC by Various Synthesis Strategies. The loading of Pt NPs onto the VC was realized through various synthesis strategies, namely, urea-assisted HD-EG using EG as reducing agent, conventional impregnation−$NaBH_4$ reduction, and MW-assisted polyol process using EG as reducing agent (i.e., EG-MW). For the urea-assisted HD-EG approach, the molar ratio of urea to Pt was fixed at 20.

Figure 3 shows HRSEM and HRTEM images for the Pt(60 wt %)/VC catalysts synthesized by the various strategies. Larger Pt NPs along with some particle agglomeration and broader size distribution were observed for the catalyst prepared by $NaBH_4$ reduction compared with the one formed by HD-EG, proving that it is hard to control the particle size and size distribution through $NaBH_4$ reduction due to its strong reducing ability at room temperature. In addition, a local pH increase in the solution

(40) Chen, X.; Chu, W.-S.; Wang, L.; Wu, Z.-Y. *J. Mol. Struct.* **2009**, *920*, 40–44.

may be involved during the synthesis process, resulting in uneven dispersion of Pt NPs. For an EG-MW process, the Pt NPs observed were more uniform in size and particle dispersion, although the particle size was slightly larger than that of the catalyst produced by $NaBH_4$ reduction. The more uniform size and particle dispersion are probably attributable to *in situ* generation of reducing agent at high temperature through the reaction shown in eq 5. As for commercial Johnson Matthey (JM) catalyst, smaller Pt NPs were observed compared with the catalysts prepared by $NaBH_4$ reduction or by EG-MW, probably due to better control of the size during the catalyst synthesis. However, the JM catalyst still shows larger Pt NPs, broader size distribution, and more agglomeration compared with the catalyst synthesized by the HD-EG strategy, which allows the *in situ* generation of OH^- during the HD step and *in situ* generation of reducing agent during the reduction step. *In situ* generation of OH^- enables the Pt(IV) complex species to deposit homogenously with uniform size on the VC support, while *in situ* generation of reducing agent enables the reduction of the deposited Pt complex species to take place simultaneously everywhere the species exist, in great contrast to the case in which a reducing agent is introduced externally, as in the conventional impregnation−$NaBH_4$ approach, or OH^- is introduced externally as in the conventional EG-MW synthesis strategy, further guaranteeing the uniform distribution of Pt NPs on the catalyst support. As for a HD-$NaBH_4$ process, *ex situ* addition of reducing agent $NaBH_4$ does not guarantee the homogeneous reduction of Pt complex ions, and some small Pt NPs produced may easily agglomerate into large NPs during $NaBH_4$ reduction. In fact, during our experiments, it was found that although the Pt catalyst produced by HD-$NaBH_4$ shows better distribution of Pt NPs along with smaller size compared with that produced by the conventional $NaBH_4$ method, agglomeration of Pt NPs was still observed in some areas on the carbon support for the Pt catalyst produced by the HD-$NaBH_4$ approach, further confirming the necessity and priority of an *in situ* reduction step like the EG step. Due to the one-pot reduction reaction feature, the HD-EG approach allows synthesis of VC-supported Pt catalysts with high metal loading of 60 wt %, still possessing small Pt NPs size and uniform particle distribution, unlike the *ex situ* reduction process conducted under H_2 flow at higher temperature (above 200 °C) after the deposition of Pt complex species on the VC support and filtration. In the latter case, elevated temperature may result in an increase in particle size and uneven particle dispersion due to particle aggregation.

Although various strategies were used for synthesis of Pt/VC catalysts, TGA data shown in Figure 4a reveals that the actual metal loadings in all the Pt/VC catalysts are very close to the normal value of 60 wt %, suggesting that all of the synthesis strategies are efficient for fabrication of high metal loading Pt catalysts.

Figure 4b shows XRD patterns for the Pt(60 wt %)/VC catalysts synthesized by the various strategies. All the VC-supported Pt catalysts exhibit characteristics of Pt face-centered-cubic structure. The average particle sizes were calculated using a Debye−Scherrer equation from the broadening of the Pt(220) reflection[41,42] as ca. 4.1 nm for Pt(60 wt %)/VC ($NaBH_4$), 4.3 nm for Pt(60 wt %)/VC (EG-MW), 3.2 nm for JM, and 2.8 nm for Pt(60 wt %)/VC (HD-EG). The calculated sizes of Pt NPs

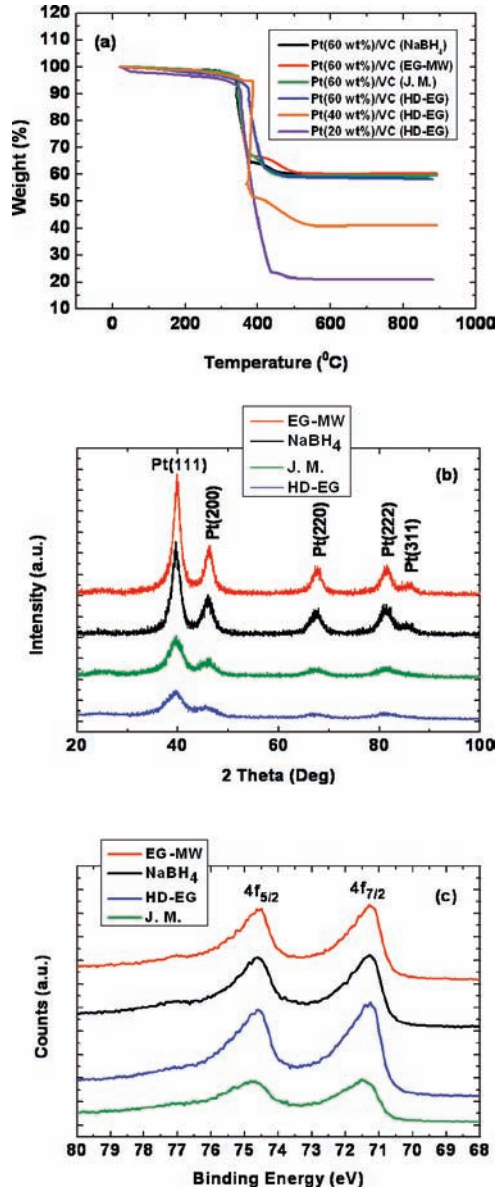

Figure 4. (a) TGA curves for Pt(60 wt %)/VC catalysts prepared by various strategies and for VC-supported Pt (20 or 40 wt %) catalyst prepared by the HD-EG strategy. (b) XRD patterns and (c) XPS spectra showing the Pt 4f region for the Pt(60 wt %)/VC catalysts prepared by various methods.

in these catalysts are in good agreement with the direct measurements from the HRSEM images shown in Figure 3.

From the XPS spectra of the Pt(60 wt %)/VC catalysts in the Pt 4f region shown in Figure 4c and Figure S3 (Supporting Information), doublet peaks were observed at 71.3 (71.5 for JM) and 74.6 eV (74.8 for JM), which are attributable to $4f_{7/2}$ and $4f_{5/2}$ of metallic Pt, respectively, implying that the dominant valences of the Pt species in the catalysts are zero. Although EG does not act as a reducing agent at room temperature, reducing species can be generated *in situ* at high temperature for reduction of metallic species, as shown in eq 5.[38] Zhou et al.[43] reported that, when the temperature of the reaction system was raised to 75 °C, only Pt^0 was observed through *in situ* NMR analysis of ^{195}Pt in the EG solution.

(41) Pozio, A.; De Francesco, M.; Cemmi, A.; Cardellini, F.; Giorgi, L. *J. Power Source* **2002**, *105*, 13–19.
(42) Tian, Z.-Q.; Jiang, S.-P.; Liang, Y.-M.; Shen, P.-K. *J. Phys. Chem. B* **2006**, *110*, 5343–5350.
(43) Zhou, Z.; Wang, S.; Zhou, W.; Wang, G.; Jiang, L.; Li, W.; Song, S.; Liu, J.; Sun, G.; Xin, Q. *Chem. Commun.* **2003**, 394–395.

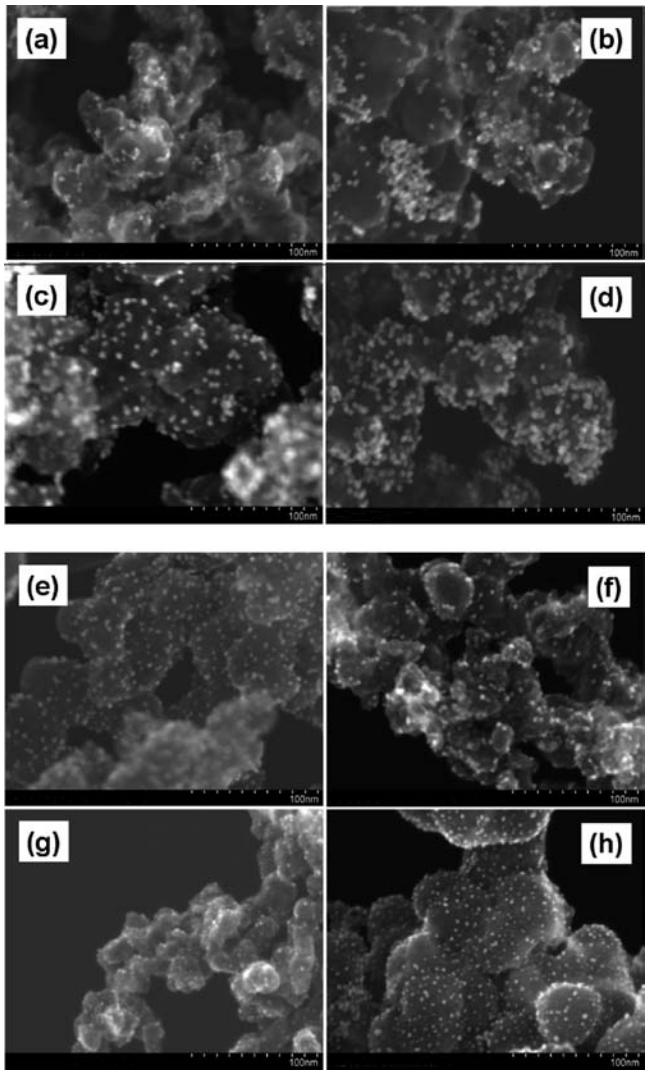

Figure 5. HRSEM images for the VC-supported Pt catalysts with metal loadings of 20 wt % (a,c,e,g) and 40 wt % (b,d,f,h) prepared by the different methods: $NaBH_4$ (a,b), EG-MW (c,d), JM (e,f), and HD-EG (g,h).

Figure 5 shows HRSEM images for the VC-supported Pt(20 wt %) and Pt(40 wt %) catalysts prepared by various strategies. The metal loadings of the Pt/VC catalysts were roughly estimated on the basis of the TGA data shown in Figure 4a and found to be very close to the normal values for these catalysts. With identical metal loading, Pt NPs are basically isolated from each other and show much smaller size with uniform dispersion in the HD-EG catalysts compared with the ones made by other methods. Particularly, the slightest increase in the size of Pt NPs was observed for the HD-EG catalysts when the metal loading was increased from 20 to 40 wt %, when compared with the catalysts made by other strategies, indicating that the HD-EG approach is a very efficient technique for the synthesis of Pt catalysts, particularly in the case of high metal loading.

At present, it remains a challenge to produce high metal loading (i.e., 60 wt %) of VC-supported Pt catalyst with small Pt NPs along with homogeneous particle distribution. Using the HD-EG strategy presented in this study, the mean size of Pt NPs in Pt(60 wt %)/VC can be tuned easily from ca. 3.3 to 2.2 nm simply by varying the amount of urea in the starting solution, followed by an EG reduction process.

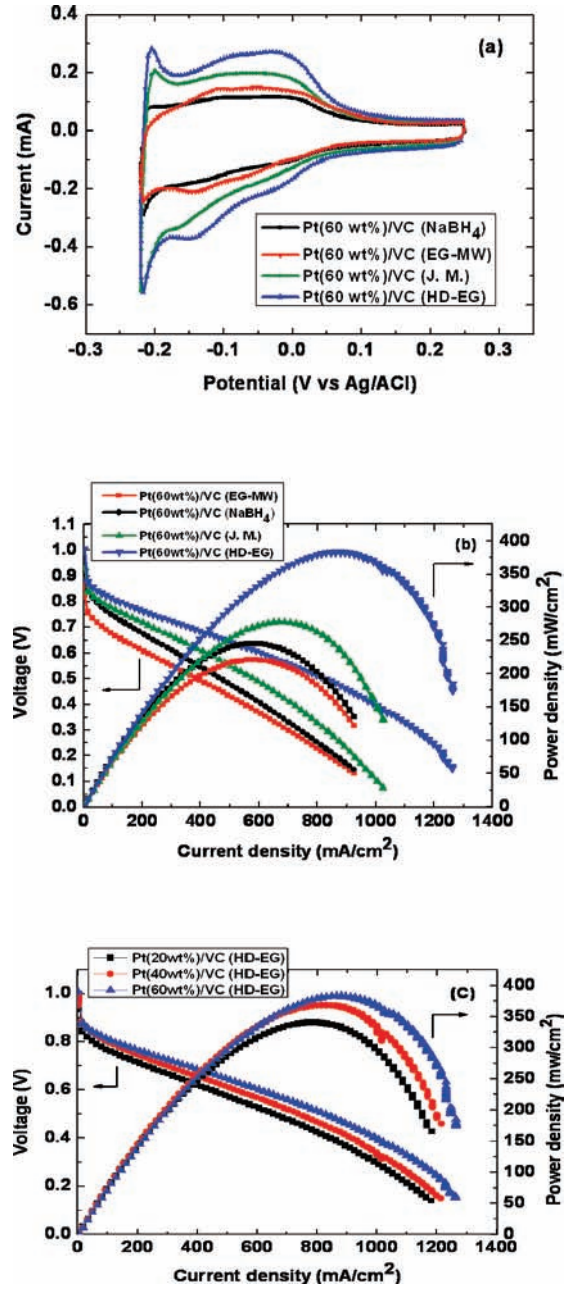

Figure 6. (a) H-electrosorption profiles in 0.5 M H_2SO_4. Fuel-cell polarization plots at 60 °C (b) for the various Pt(60 wt %)/VC catalysts and (c) for the catalysts made by the HD-EG strategy with various Pt loadings.

3.3. Pt Utilization Efficiency and Fuel-Cell Polarization Performance for Various Pt(60 wt %)/VC Catalysts. An essential and informative parameter reflecting the catalyst property is utilization efficiency, which can be calculated by dividing the electrochemical active surface area (ECSA) by the chemical surface area (CSA).

ECSA is an important measure representing the intrinsic electrocatalytic activity of Pt catalysts which can be estimated from the integrated charge (after subtraction of capacitance contribution) in the hydrogen absorption region of the steady-state cyclic voltammogram in a supporting electrolyte (i.e., 0.5 M H_2SO_4), based on a monolayer hydrogen adsorption charge of 0.21 mC/cm^2 on polycrystalline Pt. As shown in Figure 6a, well-defined hydrogen adsorption/desorption characteristics were observed for the Pt(60 wt %)/VC catalysts. A weak adsorption

peak in the potential range from +0.05 to −0.1 V and a strong adsorption peak located between −0.1 and −0.2 V were observed during the negative-going potential scan, assigned to weakly and strongly bonded hydrogen adatoms, respectively. The corresponding desorption peaks were observed during the reverse potential scan. The ECSA of Pt was determined to be 78 $m^2 g^{-1}$ for the Pt(60 wt %)/VC (HD-EG), which is much larger than that of catalysts produced by $NaBH_4$ (i.e., 35 $m^2 g^{-1}$), EG-MW (i.e., 39 $m^2 g^{-1}$), and JM one (i.e., 54 $m^2 g^{-1}$), mainly resulting from the smaller Pt NP size and uniform particle dispersion.

CSA can be calculated using the following equation: CSA $= 6000/\rho d$, where ρ represents Pt density (21.4 g cm^{-3}) and d is the average diameter of Pt NPs obtained from XRD analysis. CSA was calculated as 68 $m^2 g^{-1}$ for Pt(60 wt %)/VC ($NaBH_4$), 65 $m^2 g^{-1}$ for the EG-MW product, 88 $m^2 g^{-1}$ for the JM one, and 100 $m^2 g^{-1}$ for the HD-EG one. Thus, the corresponding utilization efficiency was ca. 51%, 60%, 61%, and 78% for the Pt(60 wt %)/VC produced by $NaBH_4$, EG-MW, JM, and HD-EG, respectively. Evidently, the highest utilization efficiency of Pt(60 wt %)/VC (HD-EG) is mainly attributable to the smaller Pt NPs and particularly the better particle dispersion, which enable more Pt NPs to work as the active sites for the desired reactions. Higher utilization efficiency is supposed to endow Pt(60 wt %)/VC (HD-EG) with higher ORR activity and improved PEMFC performance.

Figure 6b shows the polarization performance of PEMFCs at 60 °C using various Pt(60 wt %)/VC cathode catalysts. In principle, H_2-fueled fuel-cell polarization at low current density is electrochemical-activation-controlled and mainly attributed to the sluggish ORR at the cathode surface. The lowest loss in polarization voltage was observed for the HD-EG catalyst compared to the others, indicating the highest electrocatalytic activity toward ORR. The maximum power density is 384 mW cm^{-2} for the HD-EG catalyst, which is much higher than that observed for the $NaBH_4$ (245 mW cm^{-2}), EG-MW (230 mW cm^{-2}), and JM ones (278 mW cm^{-2}). The HD-EG catalyst also shows the highest electrochemical stability, as is evident in Figure S4 (Supporting Information). The higher catalytic activity and fuel-cell polarization performance demonstrated by the HD-EG catalyst are attributable to its larger ECSA and higher Pt utilization efficiency, both of which are closely related to the smaller Pt NPs and more uniform particle dispersion on the VC support.

3.4. Influence of Pt Loading on Fuel-Cell Polarization Performance. Generally, it is agreed that PEMFC polarization performance degrades with increasing Pt loading on the catalyst, particularly at low catalyst loading density (i.e., 0.2 mg of Pt cm^{-2}) at cathode. Qi et al. reported that the commercial E-TEK catalyst Pt(40 wt %)/VC shows worse PEMFC performance than the Pt(20 wt %)/VC (E-TEK) due to the much smaller Pt ECSA of the former.[44] Similar trends were also observed in our study for the $NaBH_4$, EG-MW, and JM catalysts, as shown in Figure S5 (Supporting Information). When Pt loading was varied from 20 to 60 wt %, the decrease in the maximum power observed was ca. 22%, 29%, and 20% for the $NaBH_4$, EG-MW, and JM catalysts, respectively, which is mainly attributable to the considerable increase in the Pt NPs' size and worse particle distribution, as evident from the TEM and SEM images shown in Figures 3 and 5, resulting in drastic decreases in the Pt ECSA and utilization efficiency. Interestingly, the HD-EG catalysts show a greatly different trend in Figure 6c from that shown by the other catalysts. When the Pt loading in the catalyst increases from 20 to 60 wt %, the maximum power density increases by ca. 12%. The improvement in PEMFC performance can be explained as follows. Although the increase in Pt loading in the HD-EG catalysts is large, the Pt NPs' size does not increase much. The XRD patterns shown in Figure S6 (Supporting Information) reveal a mean size of Pt NPs of 2.3, 2.6, and 2.8 nm for Pt loadings of 20, 40, and 60 wt %, respectively. Furthermore, the dispersion of the Pt NPs on the VC remains highly homogeneous, even at Pt loading up to 60 wt %. The slight increase in the Pt NPs' size may result in a limited decrease in the catalytic activity due to the decreased Pt ECSA. However, PEMFC polarization performance can be greatly improved due to the considerable reduction in the thickness of cathode, facilitating fast mass transport which enhances Pt utilization efficiency. From Figure 6c, it was interesting to notice that, even in the low or very low current region, high metal loading catalysts outperform the ones with low metal loadings. On the basis of the experimental data and our knowledge of electrochemistry, we think the main reason for this is probably the much higher electrical conductivity of Pt than that of Vulcan carbon, resulting in higher electrical conductivity of Pt(60 wt %)/VC than that of Pt(20 wt %)/VC. In addition, the thinner catalyst layer in the electrode provided by the former catalyst also contributes smaller resistance, resulting in a smaller voltage drop. Both factors favor better fuel-cell polarization performance, even in the low current region.

It is of particular importance and significance that the high Pt loading (i.e., 60 wt %) catalyst possesses enhanced fuel-cell performance compared with the Pt catalysts with moderate (i.e., 40 wt %) and even low loadings (i.e., 20 wt %). In this case, the cost of fabricating the fuel cell can be lowered due to the reduced amount of requirement of catalyst support. Furthermore, the decrease in weight and size of the fuel-cell stack not only favors high fuel efficiency but also extends applications of fuel cells.

4. Conclusions

In this study, a novel facile and simple approach, HD-EG, has been explored for synthesis of VC-supported Pt catalysts with controllable Pt NPs size. The HD-EG strategy realizes homogeneous deposition of Pt complex species on the VC through the *in situ* hydrolysis of urea and homogeneous reduction guaranteed by *in situ* generation of reducing species by EG. The size of Pt complex species and metal NPs can be controlled simply by varying the amount of urea in the starting solution. Due to the steric contraction and electrostatic charge effects, the size of Pt complex species on the VC decreases with increasing amount of urea.

In particular, the HD-EG strategy allows efficient synthesis of high Pt loading catalyst with small NPs size and uniform particle dispersion. Compared with the catalysts produced by other methods, such as $NaBH_4$ or EG-MW, the HD-EG catalysts show more homogeneous dispersion of small Pt NPs, higher ECSA, and greater Pt utilization efficiency. The HD-EG Pt(60 wt %)/VC not only outperforms catalysts with the same Pt loading prepared by other methods but also demonstrates enhanced fuel-cell polarization performance compared with the HD-EG catalysts with moderate to low metal loadings (i.e., 40 and 20 wt % Pt), even at a low catalyst loading of 0.2 mg of Pt cm^{-2}, which can facilitate the commercialization of PEMFCs.

(44) Qi, Z.-G.; Kaufman, A. *J. Power Sources* **2003**, *113*, 37–43.

The results presented in this study are highlighted as follows: improved electrocatalytic activity, utilization efficiency, and polarization performance of high Pt loading (i.e., 60 wt %) catalyst via tunable control over size and distribution of Pt NPs realized mainly by the amount of urea added in the starting solution, and further guaranteed by *in situ* reduction of Pt complex species in the EG process. The HD-EG strategy is simple and cost-effective, allowing one-pot mass production of Pt catalyst. It is also expected to be efficient for preparation of other Pt-based alloy catalysts and catalysts of metal NPs deposited on other support materials (such as CNTs). This further research is in progress. In addition, the HD-EG strategy is expected to be effective for fabrication of metal NPs without support for some specific applications where a desired metal NPs' size and size distribution are also important.

Acknowledgment. The authors thank KETEP and WCU Research Program (R31-10035) for financial support and the Korean Basic Science Institute at Jeonju, Chuncheon, and Daejeon for HRSEM, HRTEM, and XRD measurements.

Note Added after ASAP Publication. The charges on the Pt complex species in reactions 2—4 and 6 and the related text were presented incorrectly in the version published ASAP October 1, 2009. The corrected version was published October 21, 2009.

Supporting Information Available: HRSEM images for the VC-supported Pt complex species produced with various amounts of urea, XRD patterns for the Pt(60 wt %)/VC catalysts prepared by the HD-EG strategy with various amounts of urea, XPS spectrum for VC-supported Pt complex species obtained in the HD step, XPS spectra and deconvoluted curves for Pt(60 wt %)/VC catalysts, chronoamperograms obtained at 0.75 V and 60 °C in O_2-fed cathode mode for the PEMFCs using various Pt(60 wt %)/VC as cathode catalysts, fuel-cell polarization plots at 60 °C for the VC-supported Pt(20−60 wt %) catalysts prepared by various methods, and XRD patterns for the VC-supported Pt catalysts with various metal loadings prepared by the HD-EG strategy. This material is available free of charge via the Internet at http://pubs.acs.org.

JA905749E